Iranian Journal of Electrical and Electronic Engineering 04 (2022) 2557
Microgrid Special Issue 2022: Operation, Control, and Applications

IUST Iran University of Science and Technology

Iranian Journal of Electrical and Electronic Engineering

Journal Homepage: ijeee.iust.ac.ir

Research Paper

Investigation of Novel Transformerless Converters for DC Microgrid: Design and Analysis

P. Biswal*, V. V. S. K. Bhajana*(CA), and P. Drabek**

Abstract: This paper proposes two new soft-switching transformerless converters with high voltage conversion ratio. These proposed converters achieve soft-switching each with a single auxiliary resonant cell. The merit of these converters is reduced switching losses with lesser number of devices. The main switching devices are turned off with zero current switching (ZCS). Apart from the soft-switching feature, the voltage conversion ratio is increased in comparison with the existing topologies. The operating principles and the simulation results on 12V/200V/500W converter system are presented in this paper.

Keywords: Conversion ratios, Transformerless converter (TLC), Zero Voltage Switching (ZVS), Zero Current Switching (ZCS), Voltage Multiplier Cell (VMC)

1 Introduction

IN last few decades, the usage of renewable energy sources such as wind and solar power, often paired with energy storage, are widely penetrated into the energy sector industries to minimize the emissions of various harmful pollutant gases. Fig. 1 shows a schematic of a DC microgrid. High gain dc-dc converters act as a medium between the load and the source and boost the low voltage (12V-60V) generated by the battery, solar photovoltaic (PV) and fuel cell to high DC voltage (200-300V). Moreover, a high gain dc-dc converter in a DC microgrid maintains the dc-link voltage to the desired value.

Iranian Journal of Electrical and Electronic Engineering, 2022.
Paper first received 09 Jun 2022, revised 16 Dec 2022, and accepted 18 Dec 2022.
* The authors are with the School of Electronics Engineering, KIIT University, Bhubaneswar, Odisha, India.
E-mails: pravat.biswalfet@kiit.ac.in, and bvvs.kumarfet@kiit.ac.in.
** The authors are with the Regional Innovation Centre for Electrical Engineering, University of West Bohemia, Pilsen, Czech Republic.
E-mail: drabek@fel.zcu.cz.
Corresponding Author: V. V. S. K. Bhajana.
https://doi.org/10.22068/IJEEE.18.4.2557.

In present grid connected solar photovoltaic systems, a number of challenges are still left to be overcome, like weight, volume, cost and reliability of power converters and their associated systems which can be overcome by the application of newly designed and developed high power density DC-DC converters.

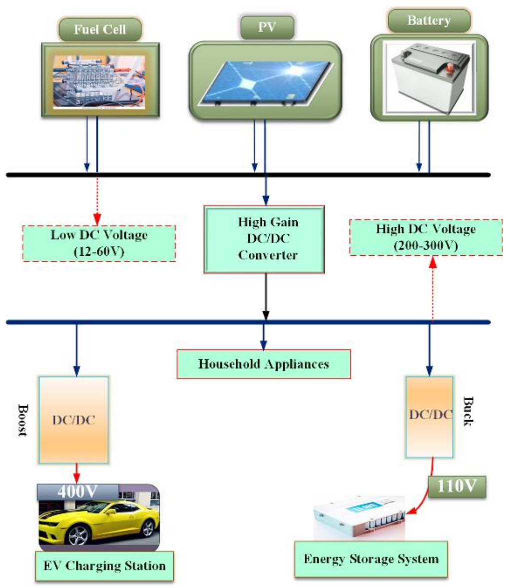

Fig. 1 General structure of DC microgrid.

In recent years desired conversion ratios in renewable energy applications are obtained using non-isolated DC-DC/High gain converters. Earlier, boost converter with bipolar voltage multiplier [1] which has significant merits such as reduced device stress, reduced output ripple, and high gain, was used. A switched-capacitor voltage multiplier (SC-VM) based boost converter [2, 3] was developed prioritizing reduction in input current ripple while obtaining high gain. However, component count is increased and the obtained voltage gain is less when compared with the then existing topologies. On the other hand, limiting the duty cycle of the switches is foremost objective in boost converters, which was achieved by incorporating the three winding coupled inductor [4, 5], two winding coupled inductor [6], and another high gain converter in addition with input coupled inductor, a voltage multiplier with incorporated with a coupled inductor [7]. Furthermore, in order to reduce voltage stresses and minimal duty cycles, converters with SC-VM [8] and without voltage multiplier cell [9] are realized.

These converters utilize extra switches, diodes and an inductor in addition with the main switching devices, to attain desired gain values. To improve the overall gain as compare with existing converters, passive, active switched inductor and switched capacitor cells [10-13] are used. However, complexity in design, cost and overall volume were the drawbacks. In the present scenario, transformerless converters (TLCs) with soft-switching operations like zero voltage switching (ZVS) and zero current switching (ZCS) are promising solutions to achieve reduced switching losses, minimized reverse recovery problems and better efficiency. To obtain high gain, additional voltage multiplier cells are used. Soft-switching capability of main switches and diodes were realized through a coupled inductor and auxiliary switches [14-17]. Though these both topologies achieve ZVS and ZCS conditions, the total number of components was drastically increased. On the other hand, usage of active clamped circuits [18] along with the coupled inductors [19] and built-in transformer [20] based converters were realized with ZVS capability. Minimization of auxiliary devices, obtaining soft-switching and improving gain are the merits of the proposed TLCs. The proposed configurations are shown in Fig.2 (a, b).

This paper presents new soft-switched transformerless converter (TLC) with a simple auxiliary cell and a VMC. The operating principles and description are explained in Section 2. The gain analysis is described in Section 3 and simulation results of the proposed converters are presented in Section 4.

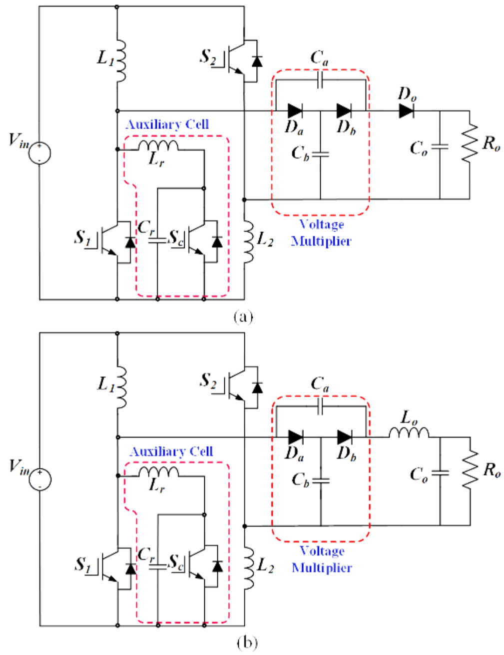

Fig. 2 Proposed converters (a) TLC-1 (b) TLC-2.

2 Operating Principles and Description

The soft-switching transformerless converters (TLCs), TLC-1 shown in Fig. 2 (a) and TLC-2 shown in Fig. 2 (b) they are comprised of two main inductors L_1, L_2, two main switches S_1, S_2 and a voltage multiplier with two diodes and two capacitors. In addition to the main components, an auxiliary switch S_c, a capacitor C_r and a resonant inductor L_r are included. The difference between topologies TLC-1 and TLC-2, is that the output diode D_o in the topology-1 is replaced with L_o in TLC-2. The key waveform for TLC-1 is shown in Fig.3 and equivalent circuits with current flow direction for the intervals (t_0-t_1) and (t_1-t_2) are shown in Fig. 4 (a, b) and Fig. 5 (a) shows for both the interval (t_2-t_3) and (t_3-t_4), Fig. 5 (b) shows for interval (t_4-t_5) and Fig. 5 (c) shows for interval (t_5-t_6), respectively. Operation for topology-2 is similar to topology-1, except the way of achieving soft-switching.

Interval (t_0-t_1): At t_0, IGBT S_c is in off condition and IGBTs S_1, S_2 are already turned off. During this interval, voltage across S_1 decreases linearly and S_2 voltage increases linearly. At t_1, the voltage across S_2 is zero and L_r current is also zero. The current and voltage equations of L_r and C_r are expressed as:

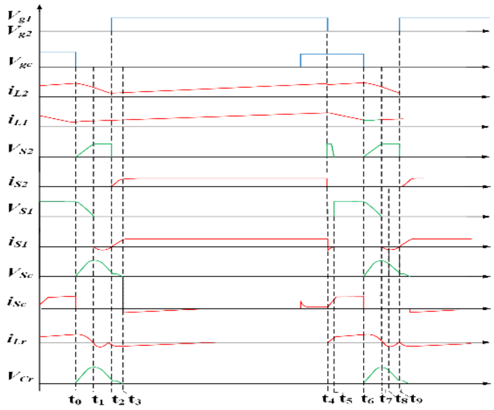

Fig. 3 Key waveform: TLC-1.

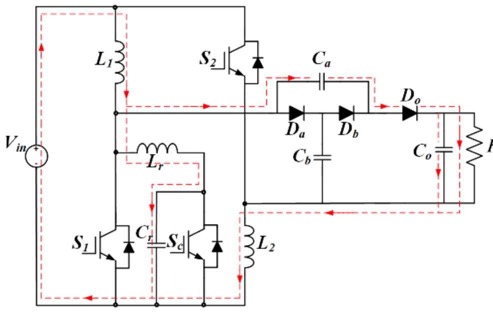

(a)

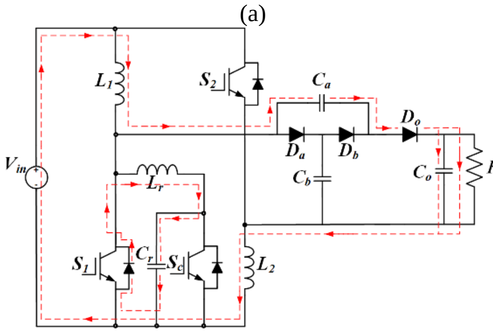

(b)

Fig. 4 Equivalent circuits (a) Interval (t_0-t_1) (b) Interval (t_1-t_2).

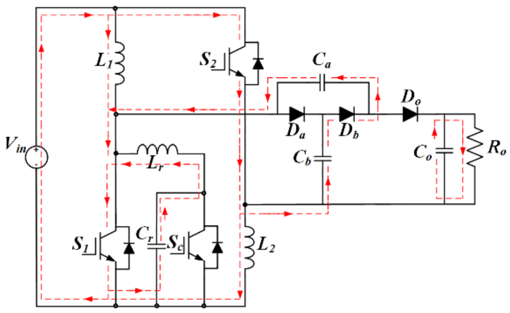

(a)

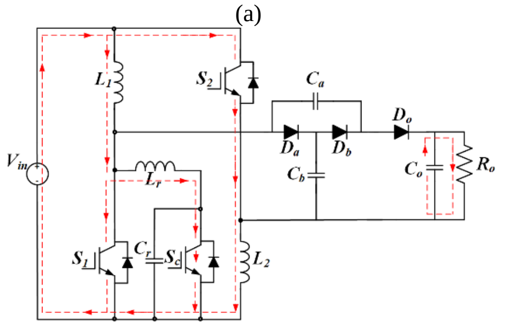

(b)

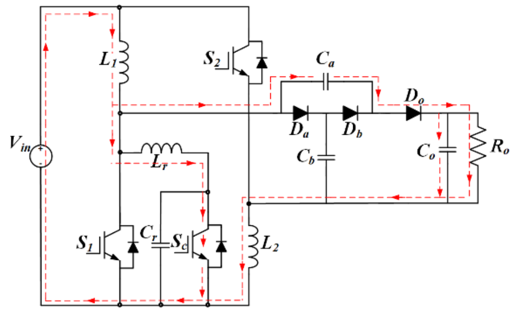

(c)

Fig. 5 Equivalent circuits (a) Interval (t_2-t_3) & (t_3-t_4) (b) Interval (t_4-t_5) (c) Interval (t_5-t_6)

$$i_{Lr}(t) = i_{Lr}(t_0)\cos\omega(t-t_0) \tag{1}$$

$$V_{Cr}(t) = I_{Lr} Z \sin\omega(t-t_0), \quad \omega = \frac{1}{\sqrt{L_r C_r}}; Z = \sqrt{\frac{L_r}{C_r}} \tag{2}$$

$$V_{Cr} = \frac{\alpha I_{in}}{V_o}\sin\omega(t-t_0) \tag{3}$$

Interval (t_1-t_2): At t_1, C_r is charged to peak level which is equal to V_o, current through L_r is zero and V_{S1} is zero. The body diode of IGBT, S_1 starts conducting. Hence, ZVS condition is achieved. Throughout this interval, the L_r current gradually decreases in reverse direction and C_r also discharges. At t_2, voltage across S_2 and L_r current will be zero and C_r gets completely discharged.

Interval (t_2-t_3): At t_2 gate signals are applied to S_1, S_2. At instant t_2, current and voltages of S_1, S_2 are zero and hence, the soft-switching condition, zero voltage zero current (ZVZC) is obtained. After a short period, current through S_1, S_2 rises to a constant value, which equal to input current. During this interval, the energy accumulates in L_1, L_2. The equations of L_r and C_r are expressed as:

$$i_{Lr}(t) = i_{Lr}(t_1)\cos\omega(t-t_1) \tag{4}$$

$$V_{Cr}(t) = -Z\sin\omega(t-t_2) \tag{5}$$

$$V_{Cr} = -\frac{\alpha I_{in}}{V_o}\sin\omega(t-t_0) \tag{6}$$

Interval (t_3-t_4): At t_3, S_c is turned on and current through L_1, L_2 linearly increase.

Interval (t_4-t_5): This is a short interval, that begins when S_1, S_2 turn off. The currents through IGBTs, S_1, S_2 reaches to zero. The diode of IGBT S_1 is conducts throughout this interval. Hence, the zero current switching (ZCS) is obtained for the IGBTs S_1, S_2.

Interval (t_5-t_6): At t_5, S_c is still in conducting state and L_2 current starts decreasing. The current through S_2 is zero and its voltage is also zero, hence ZVZCS condition is achieve. Interval (t_6-t_9): This interval is same as t_0-t_2.

3 Steady State Analysis

The following assumptions are considered for the steady state analysis

1. The IGBTs S_1, S_2, S_c and diodes D_1, D_2, D_o are ideal devices.
2. Short time intervals t_0-t_2 and t_3-t_4 are neglected.
3. The currents of the inductances L_1, L_2 are constant during t_0-t_2.

3.1 Voltage Gain

By applying KVL during t_0-t_1 and t_1-t_2, equations (7) (8), (9) and (10) are obtained.

$$V_{L1(ON)} = V_{in} \tag{7}$$

$$V_{L2(ON)} = V_{in} \tag{8}$$

$$V_{in} + V_{Cb} = V_{Ca} \tag{9}$$

$$V_{Lo} = V_{Cb} - V_{Co} \tag{10}$$

During t_3-t_4, all switches are in off state, and the voltage across inductor L_1 is,

$$V_{L1(OFF)} = \frac{V_{in} - V_{Cb}}{2} \tag{11}$$

By applying KVL in state t_3-t_4, equations (12) and (13) are obtained

$$V_{Ca} + V_{Cb} = V_{Lo} + V_{Co} \tag{12}$$

$$V_{Lo(OFF)} = V_{Ca} + V_{Cb} - V_{Co} \tag{13}$$

Volt-second balance across output filter inductor (L_O) is:

$$V_{LO(ON)}D + V_{LO(OFF)}(1-D) = 0 \tag{14}$$

Equations (10) and (12) in equation (13), gives,

$$(V_{Cb} - V_{Co})D + (V_{Ca} + V_{Cb} - V_{Co})(1-D) = 0 \tag{15}$$

After simplifying equation (9), equation (16) is obtained.

$$V_{Cb} + V_{Ca}(1-D) = V_{Co} \tag{16}$$

where:

$$V_{Ca} = V_{in} + V_{Cb} \tag{17}$$

The voltage of the multiplier cell capacitor, C_b can be written as:

$$V_{Cb} = \frac{V_o - V_{in}(1-D)}{2-D} \tag{18}$$

As per volt-second balance condition across L_1 gives.

$$V_{L1(ON)}D + V_{L1(OFF)}(1-D) = 0 \tag{19}$$

The gain expression is obtained for TLC-1 is obtained from equations (10), (18) and (19) as follows:

$$\frac{Vo}{Vin} = \frac{3+D}{1-D} \tag{20}$$

Similarly, the gain expression (21) is obtained for TLC-2, which is shown in Fig. 1 (b). TLC-1 with diode capacitor filter having gain value 19 is shown in Fig. 1 (a). TLC-2 with output L_o, C_o filter having gain value above 12 is shown in Fig. 1 (b).

$$\frac{Vo}{Vin} = \frac{3-D}{1-D} \tag{21}$$

4 Simulation Results

This section presents the performance of the proposed converters and soft-switching at light and heavy loads is validated and presented. The parameters are considered for design simulation are mentioned in Table-I. Initially, simulations are carried out on TLC-1 and the obtained results for V_{S1}, i_{S1}, V_{S2}, i_{S2}, V_{Sc} and i_{Sc} are shown in Fig. 6 (a), (b), (c), (d), (e), (f). Fig. 7 (a), (b), (c) shows the waveforms of i_{L1}, i_{L2} and i_{Lr} of the input inductors L_1, L_2, L_r and resonant capacitor, C_r, V_{Cr} is shown in Fig. 7 (d). It is also observed from the waveforms, the resonating conditions are very similar to the theoretical expectations. The voltage and current waveforms of D_a,D_b, are shown in Fig.8 (a,b,c,d) and voltage waveforms of C_a, C_b are shown in Fig.8 (e,f). It can be seen from the obtained results that, diode D_a is turned off with zero current condition and D_b is turned on with ZVS condition. Fig. 9 (a), (b), (c), (d), (e), (f) shows the waveforms V_{S1}, i_{S1}, V_{S2}, i_{S2}, V_{Sc} and i_{Sc} for IGBTs S_1, S_2, S_c for TLC-2. Fig. 1 (b) shows TLC-2 with an output filter having L_o and C_o. However, ZVS turn on in TLC-2 is achieved with a longer duration of conduction of the body diode of S_1. S_1, S_2 and S_c.

The simulations of the proposed converter are verified up to 500 W and obtained voltage is 190 V for TLC-1 shown in Fig. 1 (a) and 150V for TLC-2 shown in Fig. 1 (b). Additional current and voltage stresses are also not present in the obtained results. These proposed topologies can withstand the soft-switching capability from light load 100W to heavy load 500W. Fig. 10 (a), (b), (c), (d) shows V_{Cr}, i_{L1}, i_{L2}, i_{Lr} waveforms of L_1, L_2, L_r and C_r. L_r current is 5 A and C_r is charged to 150V and is discharged at the end of resonating period.

Table 1 Simulation parameters

Si Number	Parameters	Symbols	Value
1	Input Voltage	V_{in}	12 V
2	Output Voltage	V_o	120 V-200 V
3	Input Inductors	L_1,L_2	100µH
4	Resonant Inductor	L_r	9µH
5	Resonant Capacitor	C_r	30nF

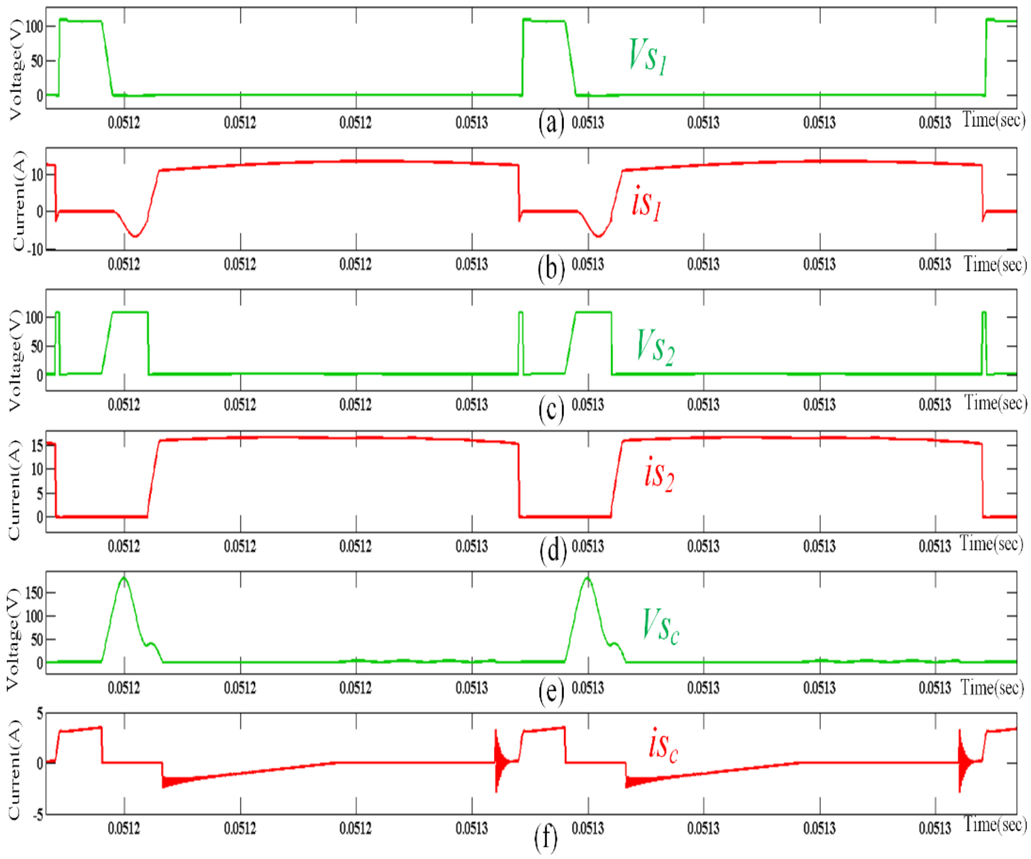

Fig. 6 Simulated Results: TLC-1 (a) V_{S1}, Collector to emitter voltage of S_1 (b) i_{S1}, Collector current of S_1 (c) V_{S2}, Collector to emitter voltage of S_2 (d) i_{S2}, Collector current of S_2 (e) V_{Sc}, Collector to emitter voltage of S_c (f) i_{Sc},, Collector current of S_c .

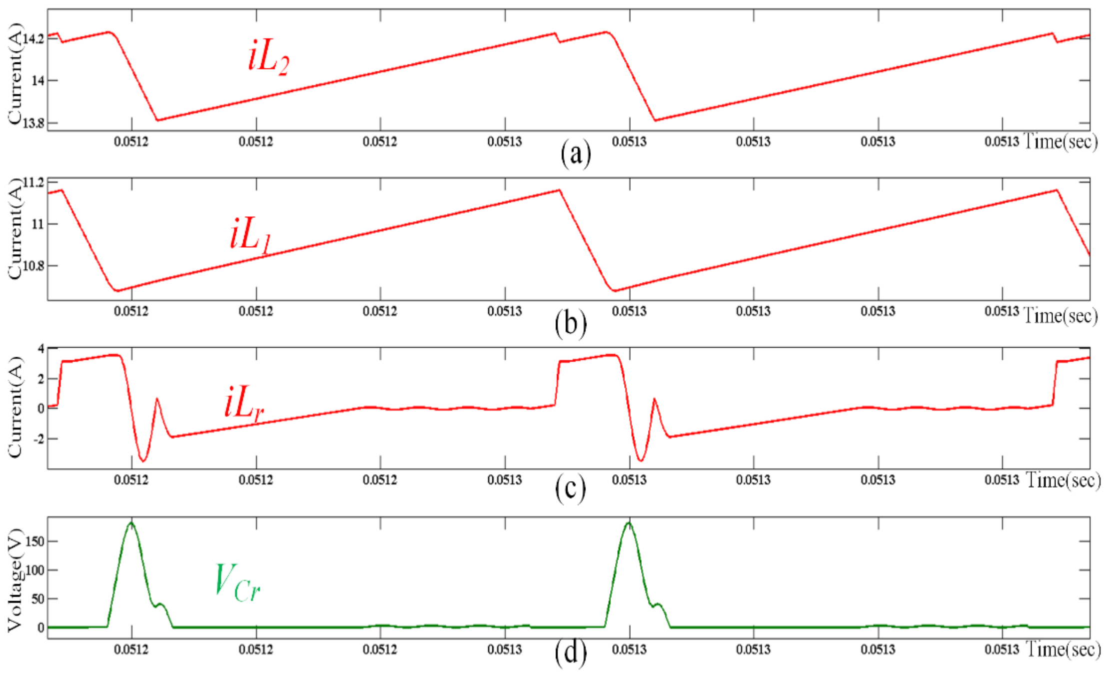

Fig. 7 Simulated Results: TLC-1 (a) Current through L_2: i_{L2} (b) Current through L_2 : i_{L1} (c) Current through L_r: i_{Lr} (d) Voltage across capacitor C_r : V_{Cr}.

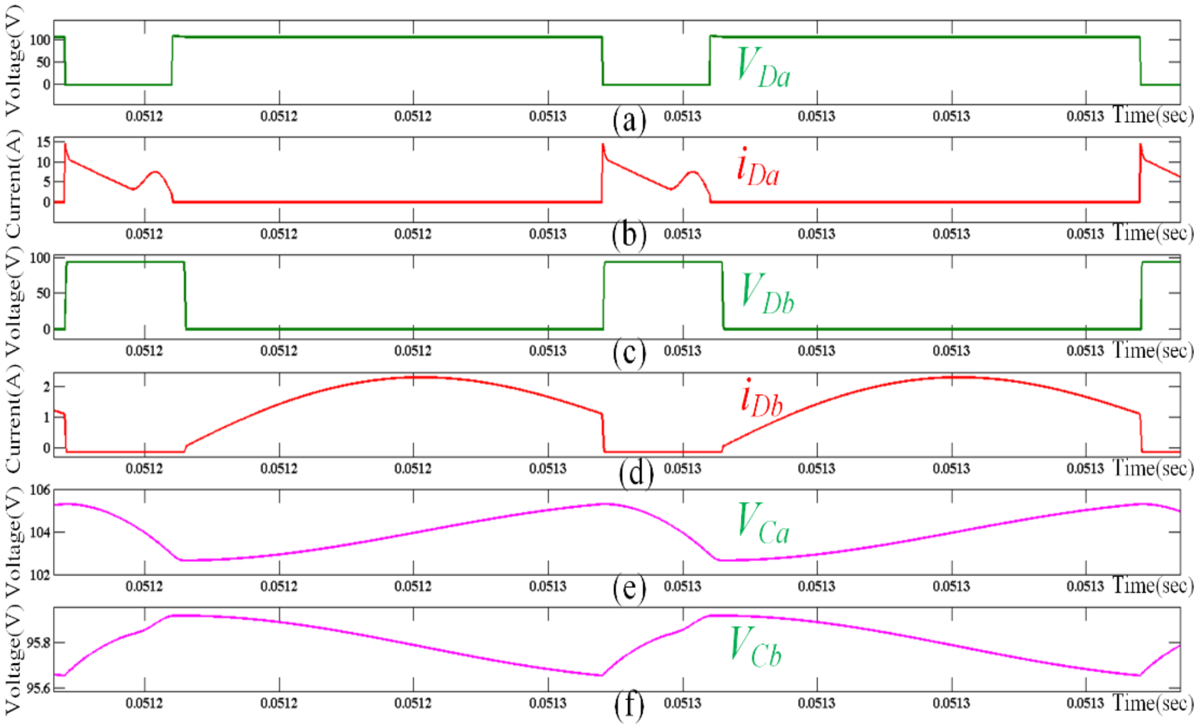

Fig. 8 Simulated Results: TLC-1 (a) Voltage across D_a: V_{Da} (b) Current through D_a: i_{Da} (c) Voltage across D_b: V_{Db} (d) Current through D_b: i_{Db} (e) Voltage across C_a : V_{Ca} (f) Voltage across C_b: V_{Cb}

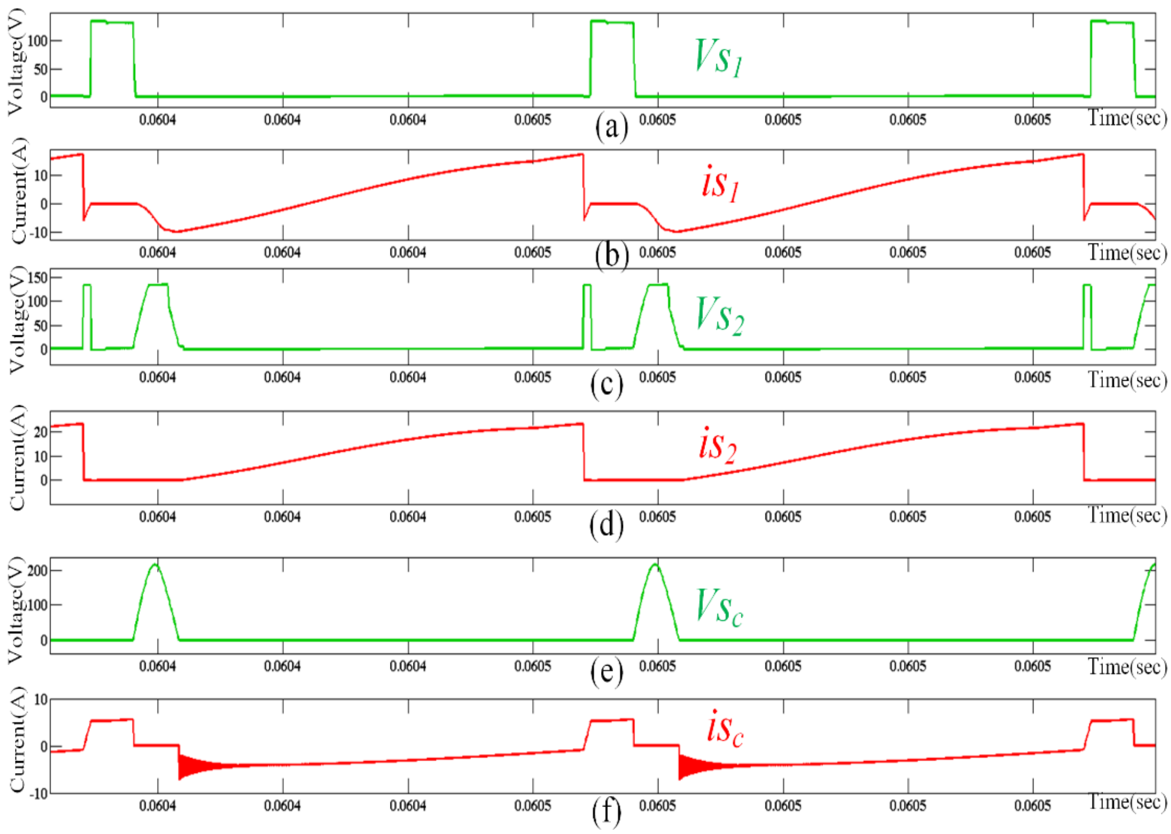

Fig. 9 Simulated Results: TLC-2 (a) V_{S1}, Collector to emitter voltage of S_1 (b) $i_{S1,}$ Collector current of S_2 (c) V_{S2}, Collector to emitter voltage of S_2 (d) $i_{S1,}$ Collector current of S_1 (e) V_{Sc}, Collector to emitter voltage of S_c (f) i_{Sc}, , Collector current of S_c

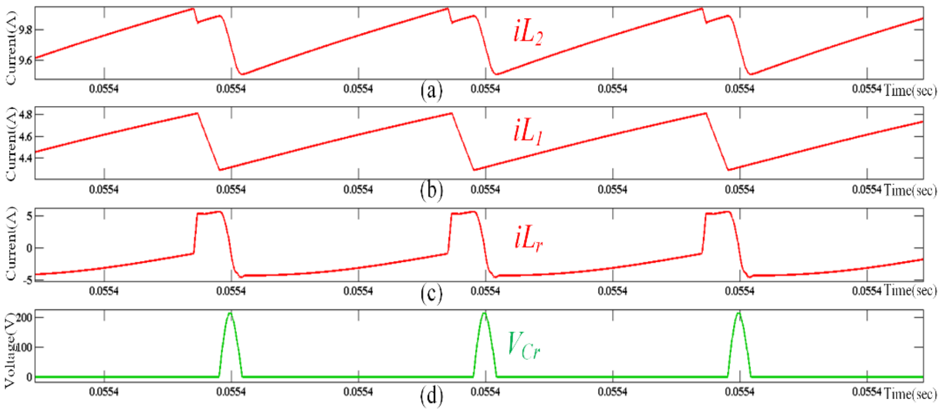

Fig. 10 Simulated Results: TLC-2 (a) Current through L_2: i_{L2} (b) Current through L_1: i_{L1} (c) Current through L_r: i_{Lr} (d) Voltage across capacitor C_r: V_{Cr}.

The voltage and current waveforms of D_a, D_b, are shown in Fig.11 (a), (b), (c), (d) and voltage waveforms of C_a, C_b are shown in Fig.8 (e) and (f). It can be seen from the obtained results that, diode D_a is turned off with zero current condition and D_b is turned on and turned off with ZCS condition. The soft turn on and turn off transitions of IGBTs S_1, S_2 are clearly seen in Fig. 12 (a), (b), (c), (d) for 450 W output power. Fig. 13 (a), (b), (c), (d) shows for 230 W. These results are observed at constant load power of 450 W. It can be seen from the obtained results is that there is an overlap between current and voltage waveforms of S_1 at light load conditions during turn on condition and duration of body diode of S_2 conduction.

These results are observed at constant load power of 500W. It can be seen from the obtained results that there is an overlap between current and voltage waveforms of S_1 at light load conditions, during turn on and during the conduction of the body diode of S_2. Similarly, for TLC-2, the soft commutation of S_1, S_2 are clearly shown in Fig. 14 (a), (b), (c), (d) for 450W output power and Fig. 15 (a), (b), (c), (d) shows the soft turn on and turn off transitions of S_1, S_2 for 230 W output power.

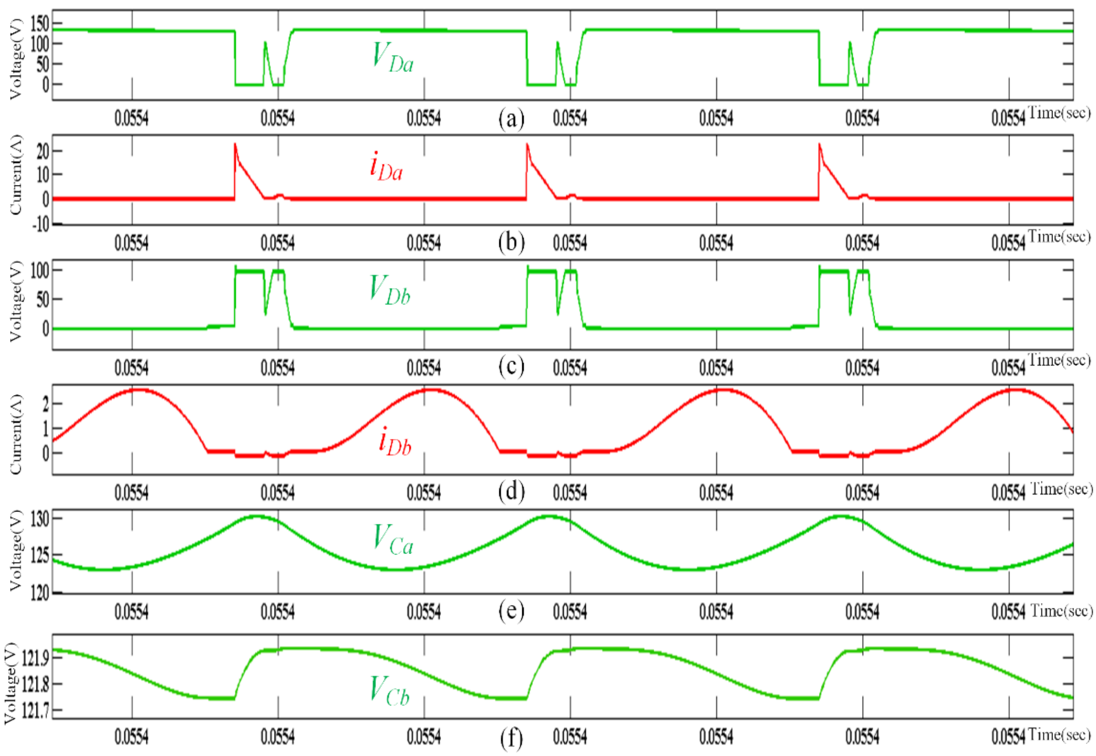

Fig. 11 Simulated Results: TLC-2 (a) Voltage across D_a: V_{Da} (b) Current through D_a: i_{Da} (c) Voltage across D_b: V_{Db} (d) Current through D_b: i_{Db} (e) Voltage across C_a : V_{Ca} (f) Voltage across C_b: V_{Cb}.

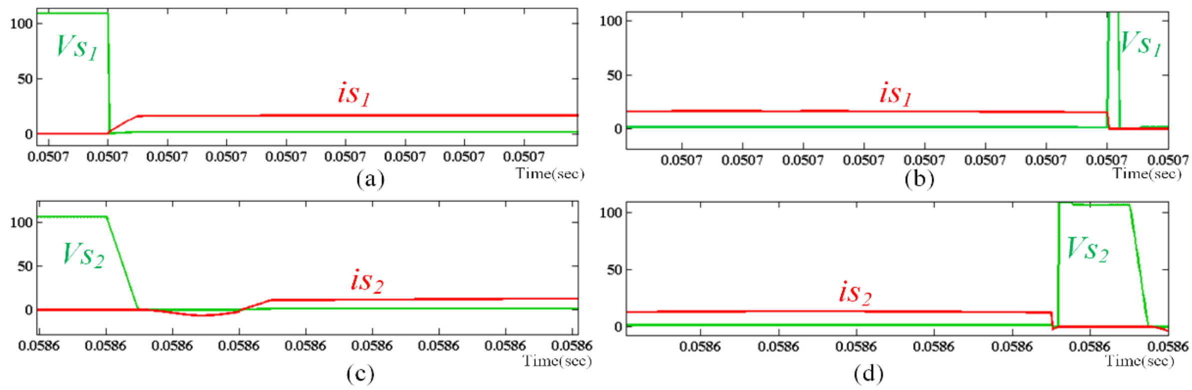

Fig. 12 Simulated Results TLC-1: Main switch transitions S_1, S_2 when converter operated at 450W output power (a) Turn-on transition of S_1 (b) Turn-off transition of S_1 (c) Turn-on transition of S_2 (d) Turn-off transition of S_2.

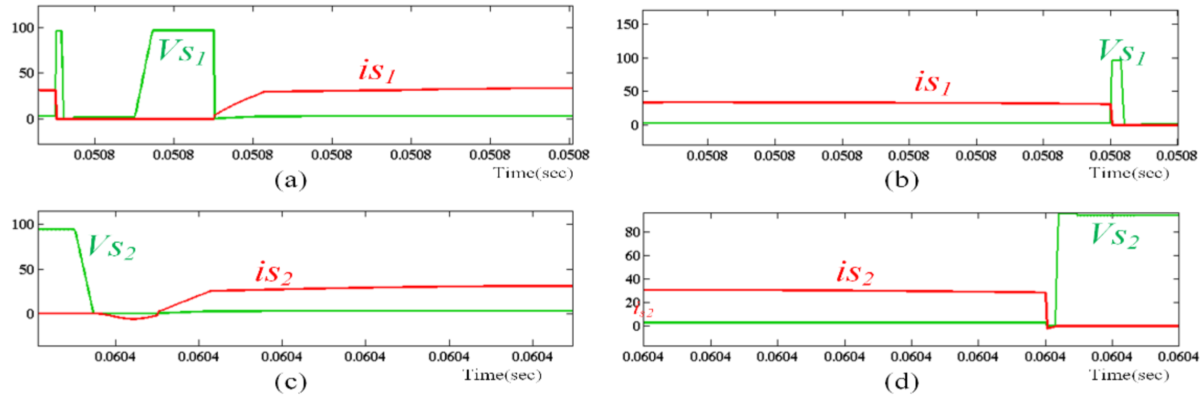

Fig. 13 Simulated Results TLC-1: Main switch transitions S_1, S_2 when converter operated at 230W (a) Turn-on transition of S_1 (b) Turn-off transition of S_1 (c) Turn-on transition of S_2 (b) Turn-off transition of S_2.

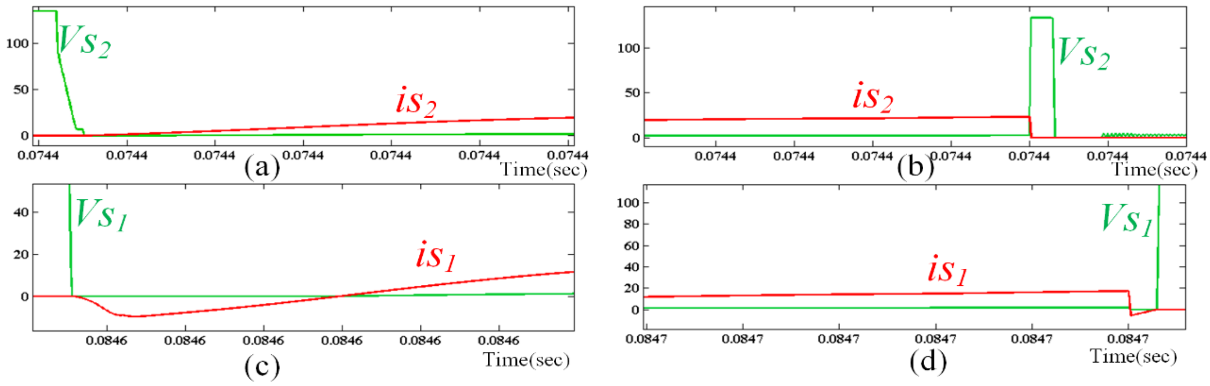

Fig. 14 Simulated Results TLC-2: Main switch transitions S_1, S_2 when converter operated at 450 W output power (a) Turn-on transition of S_1 (c) Turn-off transition of S_2 (c) Turn-on transition of S_2 (d) Turn-off transition of S_2.

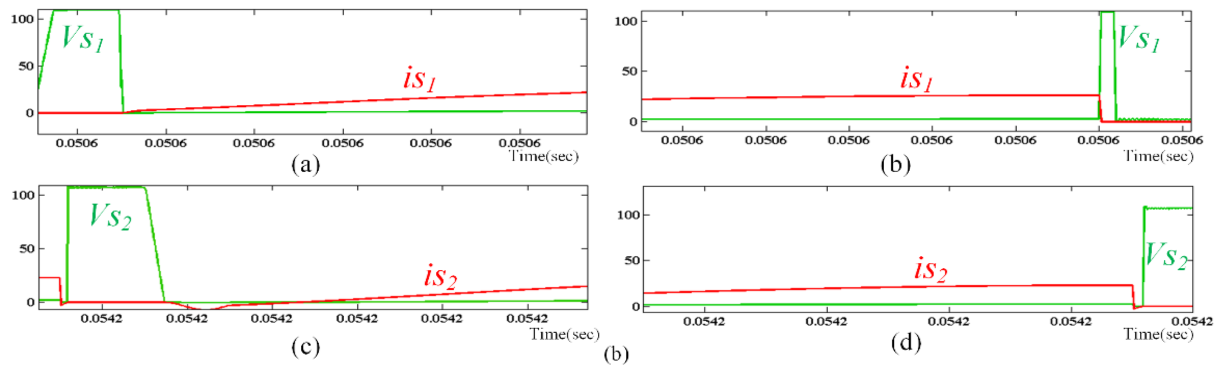

Fig. 15 Simulated Results TLC-2: Main switch transitions S_1, S_2 when converter operated at 230W output power (a) Turn-on transition of S_1 (c) Turn-off transition of S_2 (c) Turn-on transition of S_2 (d) Turn-off transition of S_2.

5 Conclusion

This paper presents two transformerless converters (TLCs) used for renewable energy applications. The operating principles and steady state analysis are also described. TLC-1, TLC-2 are designed and operated with 12 V input voltage while obtaining 200 V output voltage. For these converters TLC-1 and TLC-2, the soft-switching capability is verified at light load and heavy load conditions. ZVS turn on and ZCS turn off conditions are obtained when TLC-1 and TLS-2 are operated at 100 W and 500 W output power, respectively. The proposed two TLCs offer better solution without increasing the losses. They can provide better efficiency in high power applications with reduced number of auxiliary devices.

Intellectual Property

The authors confirm that they have given due consideration to the protection of intellectual property associated with this work and that there are no impediments to publication, including the timing to publication, with respect to intellectual property.

Funding

No funding was received for this work.

CRediT Authorship Contribution Statement

P. Biswal: Research and Investigation, Data curation, Analysis, Software and Simulation, Original Draft Preparation, **V. V. S. K. Bhajana:** Idea & Conceptualization, Research and Investigation, Software and Simulation, Methodology, Supervision, Original Draft Preparation, Revise & Editing, **P. Drabek:** Methodology, Supervision, Verification, Revise & Editing, Project Administration.

Declaration of Competing Interest

The authors hereby confirm that the submitted manuscript is an original work and has not been published so far, is not under consideration for publication by any other journal and will not be submitted to any other journal until the decision will be made by this journal. All authors have approved the manuscript and agree with its submission to "Iranian Journal of Electrical and Electronic Engineering".

References

[1] [1] B. Wu, S. Li, Y. Liu and K. Ma Smedley, "A new hybrid boosting converter for renewable energy applications", *IEEE Transactions on Power Electronics*, Vol. 31, No. 2, pp. 1203-1215, 2016.

[2] J. C. Rosas-Caro, F. Mancilla-David, J. C. Mayo-Maldonado, J. M. Gonzalez-Lopez, H. L. Torres-Espinosa and J. E. Valdez-Resendiz, "A transformer-less high-gain boost converter with input current ripple cancelation at a selectable duty cycle", *IEEE Transactions on Industrial Electronics*, Vol. 60, No. 10, pp. 4492-4499, 2013.

[3] H. Athab, A. Yazdani and B. Wu, "A transformerless DC–DC converter with large voltage ratio for MV DC grids," *IEEE Transactions on Power Delivery*, Vol. 29, No. 4, pp. 1877-1885, 2014.

[4] R. -J. Wai, C. -Y. Lin, R. -Y. Duan and Y. -R. Chang, "High-efficiency DC-DC converter with high voltage gain and reduced switch stress", *IEEE Transactions on Industrial Electronics*, Vol. 54, No. 1, pp. 354-364, 2007.

[5] M. E. Azizkandi, F. Sedaghati, H. Shayeghi and F. Blaabjerg, "A high voltage gain DC–DC converter based on three winding coupled inductor and voltage multiplier cell", *IEEE Transactions on Power Electronics*, Vol. 35, No. 5, pp. 4558-4567, 2020.

[6] M. Das and V. Agarwal, "Design and analysis of a high-efficiency DC–DC converter with soft switching capability for renewable energy applications requiring high voltage gain", *IEEE Transactions on Industrial Electronics*, Vol. 63, No. 5, pp. 2936-2944, 2016.

[7] P. Sarvghadi, A. Yazdian Varjani and M. Shahparasti, "A high step-up transformerless DC–DC converter with new voltage multiplier cell topology and coupled inductor," *IEEE Transactions on Industrial Electronics*, Vol. 69, No. 10, pp. 10162-10171, 2022.

[8] Z. Saadatizadeh, P. C. Heris, M. Sabahi and E. Babaei, "A DC–DC transformerless high voltage gain converter with low voltage stresses on switches and diodes", *IEEE Transactions on Power Electronics*, Vol. 34, No. 11, pp. 10600-10609, 2019.

[9] M. Lakshmi and S. Hemamalini, "Nonisolated high gain DC–DC converter for DC microgrids", *IEEE Transactions on Industrial Electronics*, Vol. 65, No. 2, pp. 1205-1212, 2018.

[10] Y. Tang, D. Fu, T. Wang and Z. Xu, "Hybrid switched-inductor converters for high step-up conversion", *IEEE Transactions on Industrial Electronics*, Vol. 62, No. 3, pp. 1480-1490, 2015.

[11] S. Sadaf, N. Al-Emadi, P. K. Maroti and A. Iqbal, "A new high gain active switched network-based boost converter for DC microgrid application," *IEEE Access*, Vol. 9, pp. 68253-68265, 2021.

[12] B. Axelrod, Y. Berkovich and A. Ioinovici, "Switched-capacitor/switched-inductor structures for getting transformerless hybrid DC–DC PWM converters," *IEEE Transactions on Circuits and Systems I: Regular Papers*, Vol. 55, No. 2, pp. 687-696, 2008.

[13] M. A. Salvador, J. M. de Andrade, T. B. Lazzarin and R. F. Coelho, "Nonisolated high-step-up DC–DC converter derived from switched-inductors and switched-capacitors", *IEEE Transactions on Industrial Electronics*, Vol. 67, No. 10, pp. 8506-8516, 2020.

[14] S. Khan *et al*., "A new transformerless ultra high gain DC–DC converter for DC microgrid application," *IEEE Access*, Vol. 9, pp. 124560-124582, 2021

[15] M. S. S. Andrade, T. M. K. Faistel, R. A. Guisso and A. Toebe, "Hybrid high voltage gain transformerless DC–DC converter," *IEEE Transactions on Industrial Electronics*, Vol. 69, No. 3, pp. 2470-2479, 2022.

[16] P. Mohseni, S. Mohammadsalehian, M. R. Islam, K. M. Muttaqi, D. Sutanto and P. Alavi, "Ultrahigh voltage gain DC–DC boost converter with ZVS switching realization and coupled inductor extendable voltage multiplier cell techniques", *IEEE Transactions on Industrial Electronics*, Vol. 69, No. 1, pp. 323-335, 2022.

[17] P. Mohseni, S. H. Hosseini and M. Maalandish, "A new soft switching DC–DC converter with high voltage gain capability", *IEEE Transactions on Industrial Electronics*, Vol. 67, No. 9, pp. 7386-7398, 2020.

[18] K. R. Kothapalli, M. R. Ramteke, H. M. Suryawanshi, N. K. Reddi and R. B. Kalahasthi, "Soft-switched ultrahigh gain DC–DC converter with voltage multiplier cell for DC microgrid", *IEEE Transactions on Industrial Electronics*, Vol. 68, No. 11, pp. 11063-11075, 2021.

[19] L. He, Z. Zheng and D. Guo, "High step-up DC–DC converter with active soft-switching and voltage-clamping for renewable energy systems", *IEEE Transactions on Power Electronics*, Vol. 33, No. 11, pp. 9496-9505, 2018.

[20] T. Nouri, N. Vosoughi, S. H. Hosseini, E. Babaei and M. Sabahi, "An interleaved high step-up converter with coupled inductor and built-in transformer voltage multiplier cell techniques", *IEEE Transactions on Industrial Electronics*, Vol. 66, No. 3, pp. 1894-1905, 2019.

P. Biswal was born in Bhubaneswar, India. He received the B.Tech. degree in electrical engineering from the C.V. Raman College of Engi-neering at Bhubaneshwar, Odisha, India,in 2008,and the M.Tech. degree from NIT Warangal spe-cialized in power electronics and drivein 2011.He is currently a Ph.D. Research Scholar and an Assistant Professor with KIIT University, Odisha.

V. V. S. K. Bhajana received his degrees B.E in Electronics and Communication engineering from Sapthagiri college of engineering, India (University of Madras), in 2000, M.E from the P.S.N.A College of engineering and Technology under Anna University in the year 2005 and PhD in Electrical Engineering from the Bharath University, India in 2011. He is previously associated as post-doc researcher at University of West Bohemia, Pilsen, Czech Republic during Aug 2013 to June 2015. He is currently working as Associate Professor in the School of Electronics Engineering at KIIT (Kalinga Institute of Industrial Technology) University, Bhubaneswar, India since December 2011.

P. Drabek received his M.S and PhD degrees in electrical in electrical engineering from the University of West Bohemia (UWB), Pilsen, Czech Republic, in 2000 and 2004,respectively. From 2003 to 2005, he was a Design Engineer with the company Alltronic, Ltd., Pilsen. In 2005, he joined the UWB as an Assistant Professor at the department of Electromehanics and power electronics, Faculty of electrical engineering. His main research interests include soft-switching inverters, ac-ac converters, multilevel converters and electromagnetic compatibility of power electronic converters.